Environment and Ecology 40 (4B) : 2433—2441, October—December 2022
ISSN 0970-0420

# A Green Approach for Synthesis of Titanium Dioxide Nanoparticle by *Aloe barbadensis* and its Application in Photocatalytic Decolouration of Commercial Dyes

**Riya Shah, Nirmal Kumar J. I., Nirali Goswami, Rita N. Kumar**

Received 21 July 2022, Accepted 2 September 2022, Published on 10 November 2022

## ABSTRACT

Biosynthesis of Titanium dioxide nanoparticles (TiO2NPs) is gaining popularity since it is environmentally friendly and can endure a wide range of environmental conditions. $TiO_2$NPs were produced in this study by employing *Aloe barbadensis* widely used medicinal plant. Further, synthesized $TiO_2$NPs were characterized by using microscopic techniques such as XRD (X-Ray Diffraction), EDAX (Energy dispersive X-ray microanalysis), TEM (Transmission Electron Microscopy analysis). The synthesized $TiO_2$NPs showed crystalline nature of the particle in XRD with an average size of 7.00 ± 50 nm. Whereas spherical morphology was determined by TEM. The photocatalytic decoloriation of Sudan IV, Crystal Violet (CV), Acridine Orange (AO) by using biogenic synthesized $TiO_2$NPs was evaluated under the Ultraviolet irradiation method. The synthesized $TiO_2$NPs have shown 100% of photocatalytic decolorization activity by using all three dyes dye (10–50 ppm) within 4 h incubation time.

**Keywords** Water treatment, Biogenic titanium Dioxide, Nanotechnology, *Aloe barbadensis.*

## INTRODUCTION

Water crises and pollution have become a terrifying menace to health and the environment. Increased levels of water pollutant and colouring in residual industrial waters have recently been found, which created severe health problems due to their diversity, toxicity and persistence (Rathi *et al.* 2021). Most dyes have a complicated structure and high chemical stability, allowing them to persist for long distances in flowing water, slowing photosynthetic activity, inhibiting the growth of aquatic biota by blocking out sunlight and utilising dissolved oxygen and decreasing the recreational value of the stream (Sugashini *et al*. 2022). Because of their large volume of production, sluggish biodegradation, low decolouration, and high toxicity, the breakdown of dyes in industrial wastewaters has gotten a lot of attention.

Riya Shah[1]*, Prof. Dr. Nirmal Kumar J.I.[2], Nirali Goswami[4]
[1,4]Research Scholar, [2]Head and Professor
Department of Environmental Science and Technology, Institute of Science and Technology for Advanced Studies and Research (ISTAR), A constituent college of CVM University, Vallabh Vidya Nagar 388120, Gujarat, India

Dr. Rita N. Kumar[3]
[3]HOD, Department of Biological and Environmental sciences, Natubhai V. Patel College of Pure and Applied Sciences (NVPAS), A constituent college of CVM University, Vallabh Vidya Nagar 388120, Gujarat India
Email : Shahriya1015@gmail.com
*Corresponding author

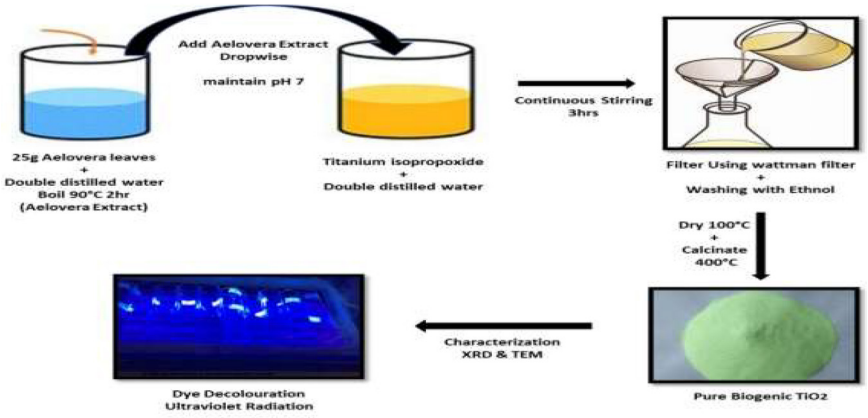


**Fig. 1.** Methodology for synthesise of biogenic $TiO_2$.

In recent years, there has been a lot of interest in heterogeneous Bio-photocatalysis employing green metal oxides such as titanium dioxide (Ikram *et al*. 2021). It has piqued the interest of researchers due to its non-toxicity, low cost, simple production, high catalytic activity, eco-friendliness and the large spectrum of metabolites released by plants also due to crystalline structure, size and area of biogenic $TiO_2$ nanoparticle it has leading potential applications in greener environmental applications (Jain *et al*. 2021). Instead of the harmful materials used in chemical and physical synthesis, green synthesis of nanomaterials utilising plants/plant component extracts has played an important role in the field of nanotechnology (Shimi *et al.* 2022). Biogenic synthesis can be done by employing reducing and capping agents derived from bacteria, fungus, yeast, algae, actinomycetes, and plants. Plant components such as leaves, bark, roots, stems, peels, and other biological resources are abundant in nature and might be used to produce harmless nanoparticles in an environmentally

**Table 1.** Langmuir adsorption isotherm.

| Dye | Intercept | Slope | qmax | KL | RL | $R^2$ |
|---|---|---|---|---|---|---|
| Sudan IV | 0.1734 | 0.1176 | 5.7670 | 1.4745 | 0.0635 | 0.9859 |
| Crystal violet | 0.2101 | 0.7690 | 4.7596 | 0.2732 | 0.2679 | 0.9633 |
| Acridine orange | 0.6103 | 0.7747 | 1.6385 | 0.7878 | 0.1126 | 0.9816 |

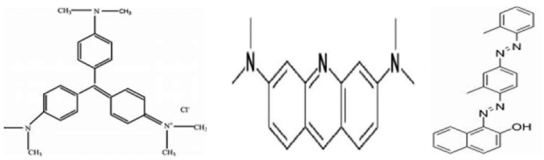

friendly manner.

In the present study the decolouration of the three toxic dyes Crystal violet, Acridine orange (AO) and Sudan IV were investigated using Ultraviolet irradiation and the Aloe Vera plant extract is used in the green synthesis of $TiO_2$ nanoparticles.

Aloe Vera is the most widely used medicinal plant. It is a succulent plant species that has been employed in herbal medicine since the early first century AD. It is a stemless plant that grows to 60–100 cm (24–39 in) tall, with thick and meaty green to grey-green leaves and white specks on the upper and lower stem surfaces. Aloe Vera Gel includes many vitamins, including vitamin B12, vitamin A, B-Group vitamins, vitamin C, vitamin E, folic acid, and 19 of the 20 amino acids required by the human body whereas Aloe is a potent detoxifier, antibacterial, nervous system tonic, immunological booster, anti-viral, and digestive aid. Aloe Vera extracts are a proven skin healer and aid in the healing of skin injuries caused by skin irritations, insect bites, burns, and wound (Lowe *et al.* 2021). Thus, using biogenic $TiO_2$ nanoparticles as a photocatalyst under ultraviolet irradiation, the effects of different operational parameters on the

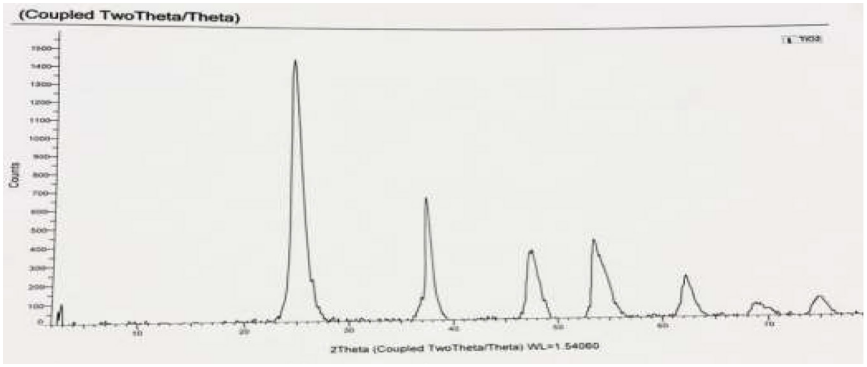


**Fig. 2.** XRD analysis of biogenic $TiO_2$.

decolouration of dyes were studied,

## MATERIALS AND METHODS

### Methodology for synthesis of biogenic $TiO_2$

Merck India Ltd supplied all of the chemicals and reagents utilized in the synthesis of TiO2 nanoparticles. The leaves were obtained from the Anand Agriculture University campus. Aloe Vera leaves were taken from the plant and properly cleansed before being chopped into little pieces. Boil 100 ml distilled water for 2 hrs at 90°C with 25g of the leaves. What man filter paper no. 41 was used to filter the extract. The filtrate was saved for nanoparticle production.

0.2 M Titanium isopropoxide (TTIP) was prepared in using double distilled water (D/W) Following adequate mixing, the aloe extract was added dropwise while constantly swirling to achieve a pH 7 solution. The mixture was continually stirred for three hours. Nanoparticles were separated using Whatman filter paper. The particles were washed with Ethanol to eliminate contaminants before being dried in a Hot Air Oven at 100°C. After thorough drying, they were calcined in a Muffle furnace at 400°C (Sunny *et al.* 2022). On calcination, a white powder of nanoparticles will develop (Fig. 1).

### Catalytic physico-chemical characterization

Synthesised biogenic nanoparticles were subjected to different sophisticated instrumental methods used for characterization are X-ray diffraction (XRD), transmission electron microscopy (TEM), EDAX (Energy dispersive X-ray microanalysis) (Kumar *et al*. 2022).

Approximately 0.5 g of the dry particles were put to a Plexiglas sample container as a randomly oriented powder, and XRD patterns were recorded between 20 and 80 angles. Anatase diffractograms were used to compare the XRD patterns. The shape and size of the particles were assessed using a transmission electron microscope (TEM) with a 100 kV accelerating voltage, model Philips Tecnai 20, Holland. For TEM analysis, the samples were put on carbon-coated copper grids. The particles were dispersed in 2-propanol to create this sample. Elemental analysis was performed using EDAX with voltage 30 kV and magnification upto 2,50,000x. All the physico-chemical characterization were performed in SICART (Sophisticated Instrumentation Center for Applied Research and

**Table 2.** Freundlich adsorption isotherm.

| Dye | Intercept | Slope | 1/n | Kf | $R^2$ |
|---|---|---|---|---|---|
| Sudan IV | 0.4836 | 0.4448 | 2.248201 | 3.045089 | 0.9747 |
| Crystal violet | 0.0305 | 0.5863 | 1.705611 | 1.072754 | 0.9063 |
| Acridine orange | 0.7909 | 2.764 | 0.361795 | 6.178741 | 0.8973 |

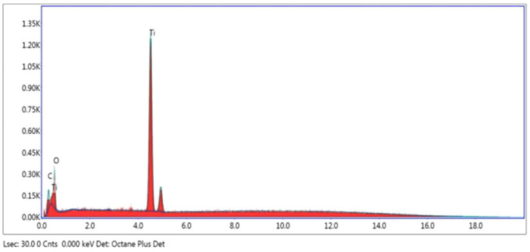


**Fig. 3.** EDAk analysis of biogenic $TiO_2$.

Testing, Vallabh Vidyanagar, Anand).

### Photocatalytic experiment

To ensure consistent dye breakdown, dye-containing flasks were kept in the dark for 30 minutes. Experiments were carried out in a 100 mL Erlenmeyer flask coated in aluminium foil to keep extraneous particles out of the dye (Soni *et al.* 2016). We looked into the impacts of dye solution concentration and catalyst dosage. Dye concentration isotherms of 10, 20, 30, 40, 50 ppm. Influencing factors such as pH, dose, and time were regulated for dye decoloration. The pH range chosen for optimization was 3, 6, 9, and 12 pH, which was determined by adding 0.1N Hcl and 0.1N NaOH. The optimal pH was determined by decoloration in natural light. $TiO_2$ nanoparticles at doses of 5, 10, 15, 20, 25 and 30 mg were added to the dye and the dose that resulted in the maximum decolouration was selected as the optimum dose. Defined volumes of Sudan IV, Crystal violet and acridine Orange were taken from flasks and placed in test tubes, each with optimized amount of the catalyst. Tubes containing catalyst were placed immediately on the UV-radiation surface. Low-pressure mercury UV tubes, each rated at 15 watts (Spectronics) generating near-ultraviolet radiation with a maximum wavelength chosen was 365 nm. The oxidation catalysed by photocatalysis when UV rays hit $TiO_2$, the process began photocatalyst. The tubes were then gently stirred to agitate them every now and then. Various factors like as temperature and pH were measured at predetermined intervals. After that, the samples were centrifuged and the results were analyzed. While the duration for $TiO_2$ nanoparticles was tuned, dye decoloration was seen under UV irradiation. Dye mineralization occurs only in the presence of a photocatalyst. At regular intervals, dye samples of 2–3 ml were taken from the test solution, centrifuged for 4–5 minutes at 950–1,000 rpm, and their absorbance was measured at 520 (Sudan IV), 690 nm (Crystal violet), 494 nm (Acridine orange) with a spectrophotometer (Alasel *et al.* 2017; Papadimitriou *et al.* 2019, Kostjukova *et al*. 2021). The photo degradation efficiency was calculated using the equation :

$$\text{Photo degradation efficiency} = \frac{\text{Initial OD–Final OD}}{\text{Initial OD}} \times 100 \quad (1)$$

## RESULTS AND DISCUSSION

### Charactrization of $TiO_2$ nanoparticles

### Xray diffraction analysis (XRD)

The pattern of biosynthesized $TiO_2$ nanoparticles is shown in Fig. 2. As XRD can determine the sample phase, phase composition, and particle size, it is

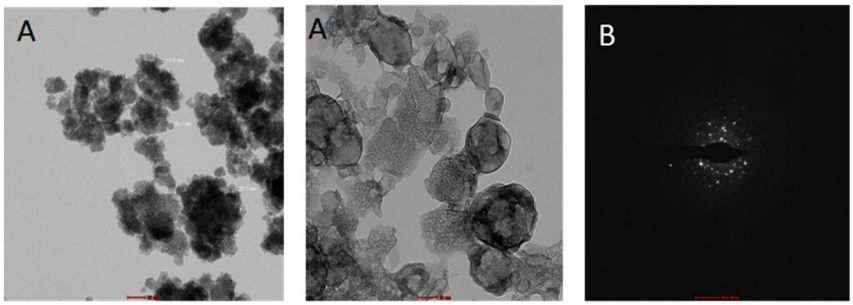


**Fig. 4.** A TEM analysis for biogenic $TiO_2$, B SAED pattern of biogenic $TiO_2$.

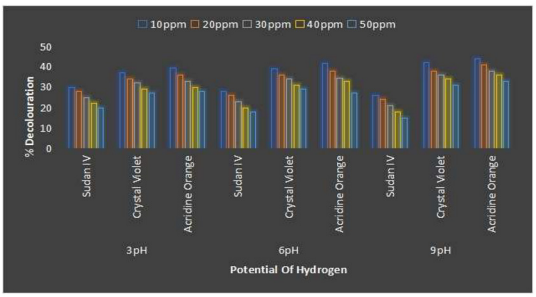


**Fig. 5.** pH optimization with reference to initial dye concentration.

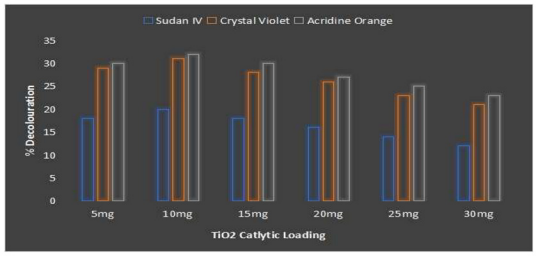


**Fig. 6.** Optimization of catalytic dosage.

regarded one of the most essential methods for crystalline material structure characterization. The spectra show the development of anatase-phase titania with diffraction angles (2θ) of at 25.24°, 37.91°, 47.92°, 54.07°, 62.59°, 69.00°, and 75.06°. Our findings are very similar to Kaur and co-workers (2021) and those of the standard JCPDS File No (21-272). From the XRD spectra, a prominent peak at 25.24° is solely related with the $TiO_2$ anatase crystallographic plane without the presence of any impurities. Diffraction line broadening occurs when the grain size is less than 100 nm. Accordingly, Scherrer's formula, which is given by equation :

$$d=k\lambda/(\beta\cos\theta) \qquad (2)$$

Where d is the crystal size; k is the wavelength of the X-ray radiation (k = 0.15406 nm) for Cukα; k is usually taken as 0.89; and b is the line width at half-maximum height, can be used to calculate the particle size of the prepared nanomaterials. the broader diffraction peaks attributed to the presence of the smaller crystallite size (Şelte *et al*. 2019), nearly 7–50 nm calculated using Scherrer's formula. The stoichiometry of the final matter is highly dependent on the restricted pressure used during the production. As a result, the stoichiometries of biosynthesized $TiO_2$ nanoparticles could be very diverse (Ansari *et al.* 2022). The presence of strong peaks supported the crystallinity of $TiO_2$ nanoparticles in the anatase form, whereas the absence of spectra represented alternative $TiO_2$ crystallite forms.

**Energy dispersive X-ray microanalysis (EDAX)**

The elemental composition of the nanoparticles can be determined through EDAX analysis. The $TiO_2$ nanoparticle includes 51.02% Titanium, 38.73 % oxygen, and 10.25 % carbon, according to the results of the examination similar results were also observed by Kaur and co-workers (2021). As a result, the Biogenic produced particles have been identified as Titanium Dioxide nano catalysts (Fig. 3). The EDAX spectrum shows that there are no further contaminants within the detection limit, indicating that the material is pure.

**Transmission electron microscopy analysis (TEM)**

TEM analysis pictures of $TiO_2$ nanoparticles generated after 12 hrs at room temperature infests the NPs were of agglomerated Irregular spherical shape (Fig. 4A) with an average size about 50 nm for biogenic synthesized $TiO_2$ respectively (Verma *et al.* 2022). The particle size of $TiO_2$ nanoparticles measured using TEM data is found to be fairly consistent with the particle size estimated using XRD examination. Figure 4B shows the $TiO_2$ nanoparticles Selected Area Electron Diffraction (SAED) pattern. The formation of $TiO_2$ nanoparticles is indicated by the presence of concentric Scherrer's rings that demonstrate orientation in all directions.

**Photocatalytic decolouration**

**Alkalinity and acidity function**

Studied the effect of change in acidity and alkalinity function with reference to initial dye concentration under normal light conditions. pH of the dye was studied as it is considered to be one of the most important parameters that can affect the photocatalytic degradation process. The initial pH of the dye was varied from

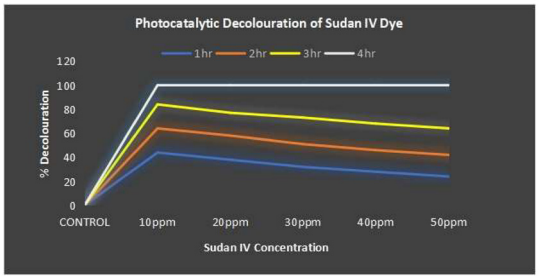


**Fig. 7.** Photocatalytic decolouration of Sudan IV dye.

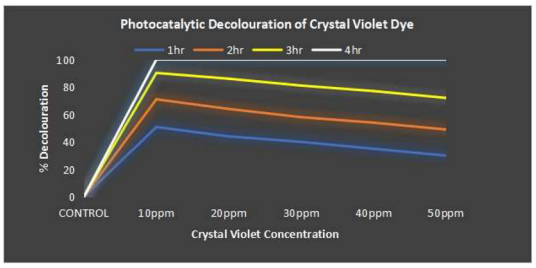


**Fig. 8.** Photocatalytic decolouration of crystal violet dye.

pH 3 to 9. Experiment on pH 12 was also carried out but cause of removal of color due to addition of NaOH it has not been taken into consideration. The studies were carried out with 10, 20, 30, 40, 50 ppm of Sudan IV, Crystal violet and Acridine orange dye solution and 5 mg catalyst dose (Fig. 5). By studying effect of pH on adsorption of Sudan IV it was found that the optimum pH for adsorption of dye is 3 (Sajjala *et al.* 2020) which was about 18%. Which confirms that Sudan IV dye has low absorption capacity in alkaline medium. For Crystal violet and Acridine Orange dye the maximum amount discoloration was obtained at pH 9 (Abbas *et al.* 2020, Hasanpour *et al.* 2020) which was 42% and 44% respectively, photocatalytic decolouration of Crystal violet and Acridine may take place in acidic pH because several hydroxyl ions increase at higher pH values which eventually leads to increase in the decolouration.

**Effect of initial dye concentration**

Initial dye concentration was also referred in the experimental design during the pH optimization by selection the concentration of 10, 20, 30, 40, 50 mg/L range where decolouration reduced with increase in concentration (Paul *et al*. 2020) (Fig. 5) as some UV light photons were absorbed by a large number of dye molecules as the dye concentration grew. The number of effective photons absorbed by the catalyst's surface was lowered. The number of excited biogenic $TiO_2$ electrons created by effective photons dropped, reducing the size of the producing electron and holes. Simultaneously, contaminants and other organic compounds were likely deposited on the $TiO_2$ surface, making it more difficult for electrons to enter the solution. As a result, less and fewer electronsentered the dye solution and reacted with adsorbed hydroxide ions to create hydroxyl radicals, the major oxidizing species responsible for organic compound photooxidation.

**Effect of catalyst loading**

After optimizing pH, the catalyst loading is another important parameter which has strong influence on the decolouration kinetics of dye solution. In order to determine the optimal amount of catalyst concentration, a series of experiments were carried out using different amount of $TiO_2$ catalyst varying from 5, 10, 15, 20, 25, 30 mg at optimized pH and initial dye concentration under normal light condition. By increasing the catalyst concentration initially from 5 mg–10 mg there was increase in the dye decolouration further analysis decrease in the decolouration was observed (Fig. 6). This enhances the fact that the surplus catalyst can scatter the photon in photoreaction system (Zeng *et al*. 2019). This could be due to activated molecules colliding with $TiO_2$ ground state molecules, deactivating them. Following these findings, it was decided to keep the amount of $TiO_2$ in further photocatalytic decolouration tests at 10 mg/L.

**Photocatalytic decolouration under ultraviolet radiation**

The decolouration of 3 organic dyes Sudan IV, Crystal violet and acridine Orange dye solution under UV light irradiation at room temperature was used to test the photo catalytic characteristics of the as-prepared samples.

Control experiments were carried out without

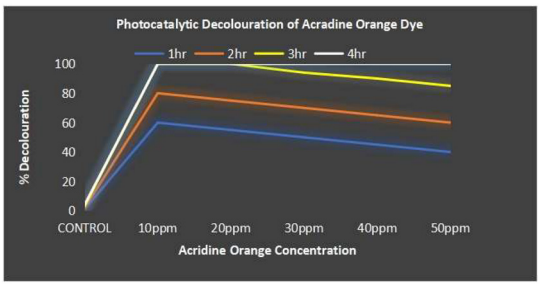


**Fig. 9.** Photocatalytic decolouration of acridine orange dye.

the addition of the catalyst to discover probable dye losses in the system. Pure catalyst $TiO_2$ was applied to varying dye concentrations in the course of photo catalytic decolouration of 3 commercial dyes. In the control experiment, no obvious loss was seen, indicating that the dyes were stable in our experiment. 100% removal was observed for all the three dyes during our experiment. Different dye concentrations (10 ppm, 20 ppm, 30 ppm, 40 ppm, 50 ppm) with optimum pH 3 for Sudan IV and pH 9 for Crystal violet and Acridine orange and optimum catalytic dose 10 mg was found to completely decolorize the dyes. For Sudan IV dye 40 and 50 ppm dye concentration about 50% decolouration was observed in 2 hrs and 100% removal for all dye concentration was observed in 4 hrs as shown in Fig. 7. Crystal violet dye nearly 90% removal was observed for 10 and 20 ppm dye concentration in 3hrs whereas,100% removal was observed even for 40 and 50 ppm dye concentration at 4hrs of irradiation (Fig. 8). The fastest decolouration observed was for Acridine orange dye out of all the three dye as 95%—90% removal for 10 and 20 ppm of dye was observed in 3hrs of irradiation with nearly 75—80% removal for 30, 40, 50 ppm of dye concentration (Fig. 9). The decolouration decreased with increase in dye concentration but 100% removal was observed with biogenic $TiO_2$ nano catalyst in 4hrs of irradiation time for all the 3 dyes.

## Adsorption isotherm

For analysing experimental equilibrium parameters, Langmuir and Freundlich models are the most widely employed isotherm equations. The Langmuir isotherm model is based on the assumption that the adsorbent's surface has a finite number of active sites that are uniformly distributed. Because these active sites have the same proclivity for adsorption as a monomolecular layer, there is no interaction between the adsorbed molecules. Adsorption isotherms depict the equilibrium relationship between the bulk activity of adsorbate in solution and the moles adsorbed onto the surface at constant temperature. The adsorption isotherm (Freundlich and Langmuir) connects the equilibrium adsorbate concentration in the bulk to adsorbate absorption on the adsorbent surface and optimally describes the adsorption characteristics for a wide range of adsorbate concentrations (Ewis *et al.* 2020).

The separation factor "RL," a significant characteristic of the Langmuir adsorption isotherm, was used to describe the affinity of nanoparticles for dye (Fegade *et al.* 2019). Sudan IV, Crystal violet, and Acridine orange dyes have RL values of 0.0635, 0.2679, and 0.1126, respectively (Table 1). The values of RL reclining in the range of 0 to 1 showed that the adsorption was favourable. The significance of the n value is that it denotes the adsorption nature in the Freundlich adsorption isotherm (Table 2). The importance of n is as follows : n = 1, adsorption is linear, n 1, adsorption is chemical, n >1, adsorption is physical. In the current investigation, the value of n in the Freundlich isotherm was determined to be in the range of 0 to 1. The value of n in the Freundlich isotherm in this investigation was found to be in the range of 0 to 2, indicating that the adsorption was physisorption for Sudan IV and chemosorption for Acridine Orange Dye, indicating that the Langmuir Adsorption isotherm was not favourable.

Both Langmuir and Freundlich values indicated that dye adsorption onto the adsorbent was fast and had a large adsorption capacity. The $R^2$ value of the graph, on the other hand, indicates the experiment's accuracy.

## Mechanism of photocatalysis

The energy of incoming UV radiation exceeds the bandgap energy of $TiO_2$NPs. When ultraviolet irradiates on the surface of $TiO_2$NPs, electrons (e–) in the conduction band (CB) and holes (h+) in the valance band (VB) are created, as shown in Fig. 10 the pho-

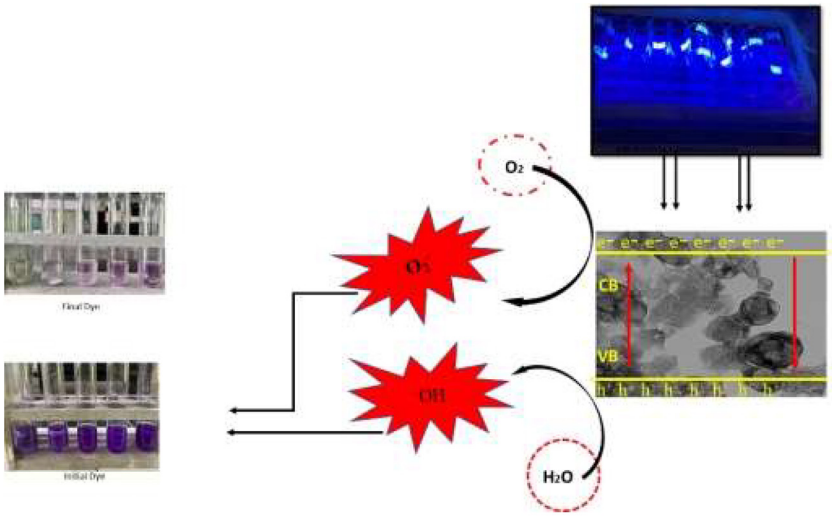


**Fig. 10.** Photocatalytic mechanism.

tocatalytic mechanism dye. e– produces superoxide free radicals (O2–) from dissolved oxygen, while h+ produces OH free radicals. As numerous studies have explained, these intermediates are highly active oxidising and reducing agents that are responsible for dye photodegradation (Vinayagam *et al.* 2021).

## CONCLUSION

The capacity of Biogenically synthesised $TiO_2$ nanoparticles for removal of commercial dyes was examined in this paper where optimization of pH, dosage plays significant role where Sudan IV dye decolouration was more efficient in acidic pH 3 and that for Crystal violet and Acridine Orange was in alkaline medium pH 9. The synthesis process was found to be important in the development of $TiO_2$ with particle sizes of 7–50 nm, respectively. It was found that $TiO_2$ has a spherical irregular morphology. Whereas the combination of Ti, O, C in EDAX analysis confirm that the particles are biogenic in nature. This biogenic catalyst synthesised from aloe extract was able to completely decolorize the dye under UV radiation in 4hrs the decolouration was observed as fast in Acridine orange and Crystal violet compared to Sudan IV. The Freundlich isotherm and the Langmuir isotherm accurately represent the data, demonstrating that adsorption by the adsorbent is favourable. According to the findings biogenic $TiO_2$ have significant promise as adsorbents for the elimination of organic dye and can be used commercially as adsorbent due to environmental friendliness.

## REFERENCES

Abbas HA, Nasr RA, Abu-Zurayk R, Al Bawab A, Jamil TS (2020) Decolourization of crystal violet using nano-sized novel fluorite structure Ga2Zr2− x W x O7 photocatalyst under visible light irradiation. *Royal Soc Open Sci* 7(3) : 191—632.

Alasel M, Keusgen M (2017) A new platform for serological analysis based on porous 3-dimensional polyethylene sinter bodies. *J Pharmaceut Biomedical Analysis* 145 :110—118.

Ansari A, Siddiqui VU, Rehman WU, Akram MK, Siddiqi WA, Alosaimi AM, Rafatullah M (2022) Green synthesis of $TiO_2$ nanoparticles using *Acorus cala*mus leaf extract and evaluating its photocatalytic and *in vitro* antimicrobial activity. *Catalysts* 12(2) : 181.

Ewis D, Benamor A, Ba-Abbad MM, Nasser M, El-Naas M, Qiblawey H (2020) Removal of oil content from oil-water emulsions using iron oxide/bentonite nano adsorbents. *J Water Process Engg* 38 : 101—583.

Fegade U, Jethave G, Su KY, Huang WR, Wu RJ (2018) An multifunction Zn0. 3Mn0. 4O4 nanospheres for carbon dioxide reduction to methane via photocatalysis and reused after five cycles for phosphate adsorption. *J Environm Chem Engg* 6(2) : 1918—1925.

Hasanpour M, Hatami M (2020) Photocatalytic performance of aerogels for organic dyes removal from wastewaters : Review study. *J Molecular Liquids* 309 : 113094.

Ikram M, Javed B, Hassan SWU, Satti SH, Sarwer A, Raja

NI, Mashwani ZUR (2021) Therapeutic potential of biogenic titanium dioxide nanoparticles : A review on mechanistic approaches. *Nanomedicine* 16 (16) : 1429—1446.

Jain A, Wadhawan S, Mehta SK (2021) Biogenic synthesis of non-toxic iron oxide NPs via Syzygium aromaticum for the removal of methylene blue. Environm Nanotechnol, Monit *Manag* 16 : 100464.

Kaur G, Kaur H, Kumar S, Verma V, Jhinjer HS, Singh J, Al-Rashed S (2021) Blooming approach : One-pot biogenic synthesis of $TiO_2$ nanoparticles using piper betle for the degradation of industrial reactive yellow 86 Dye. *J Inorganic Organometallic Polymers Materials* 31 (3) : 1111—1119.

Kostjukova LO, Leontieva SV, Kostjukov VV (2021) The vibronic absorption spectra and electronic states of acridine orange in aqueous solution. *Spectrochim ica Acta Part A : Molecular and Biomolecular Spectroscopy* 249 : 119302.

Kumar S, Sharma A, Gautam D, Hooda S (2022) Characterization of Mesoporous Materials. In Advanced Functional Porous Materials. Springer, *Chamreg* pp 175—204.

Lowe H, Steele B, Bryant J, Fouad E, Toyang N, Ngwa W (2021) Antiviral activity of Jamaican medicinal plants and isolated bioactive compounds. *Molecucules* 26 (3) : 607.

Papadimitriou M, Hatzidaki E, Papasotiriou I (2019) Linearity comparison of three colorimetric cytotoxicity assays. *J Cancer Therapy* 10 (07) : 580.

Paul JJ, Surendran A, Thatheyus AJ (2020) Efficacy of orange peel in the decolourization of the commercial auramineyellow dye used in textile industry. *Ind J Biochem Biophysics (IJBB)* 57 (4) : 481—485.

Rathi BS, Kumar PS, Vo DVN (2021) Critical review on hazardous pollutants in water environment : Occurrence, monitoring, fate, removal technologies and risk assessment. *Sci Total Environ* 797 : 149134.

Sajjala SR, Sairam V (2020) De-Colorization of Sudan IV Dye Solution by Solar Photo Fenton and $TiO_2$ Mediated Solar Photo Fenton Processes: A Comparative Study. *Int J Advan Res in Engg Technol* 11 (6) : In press.

Şelte A, Özkal B (2019) Crystallite size and strain calculations of hard particle reinforced composite powders (Cu/-Ni/Fe–WC) synthesized via mechanical alloying. *Proc Estonian Acad Sci* 68 (1) : 66—78.

Shimi AK, Ahmed HM, Wahab M, Katheria S, Wabaidur SM, Eldesoky GE, Rane KP (2022) Synthesis and Applications of Green Synthesized $TiO_2$ Nanoparticles for Photocatalytic Dye Degradation and Antibacterial Activity. *J Nanomaterials.*

Soni H, Kumar JN, Patel K, Kumar RN (2016) Photocatalytic decoloration of three commercial dyes in aqueous phase and industrial effluents using $TiO_2$ nanoparticles. *Desalination Water Treatment* 57(14) : 6355—6364.

Sugashini S, Gomathi T, Devi RA, Sudha PN, Rambabu K, Banat F (2022) Nanochitosan/carboxymethyl cellulose/ $TiO_2$ biocomposite for visible-light-induced photocatalytic degradation of crystal violet dye. *Environm Res* 204 : 112047.

Sunny NE, Mathew SS, Chandel N, Saravanan P, Rajeshkannan R, Rajasimman M, Kumar SV (2022) Green synthesis of titanium dioxide nanoparticles using plant biomass and their applications-A review. *Chemosphere* 134612.+

Verma V, Al-Dossari M, Singh J, Rawat M, Kordy MG, Shaban M (2022) A Review on Green Synthesis of $TiO_2$ NPs : Photocatalysis and Antimicrobial Applications. *Polymers* 14 (7) : 1444.

Vinayagam R, Pai S, Murugesan G, Varadavenkatesan T, Selvaraj R (2021) Synthesis of photocatalytic zinc oxide na-noflowers using Peltophorum pterocarpum pod extract and their characterization. *Appl Nanosci* 1—11.

Zeng B, Liu W, Zeng W, Jin C (2019) Carbon NanotubesWrapped Urchin-Like Bi2S3 Composites with Enhanced Photocatalytic Performance. *J Nanosci Nanotechnol* 19(4): 2276—2280.